Analysis and Optimization of Spectral and Energy Efficiency in Underlaid D2D Multi-Cell Massive MISO Over Rician Fading

Ramin Hashemi, *Graduate Student Member, IEEE*, Mohammad Kazemi, *Member, IEEE*, and Abbas Mohammadi, *Senior Member, IEEE*

***Abstract*—This paper investigates the uplink spectral efficiency (SE) characterization and energy efficiency (EE) optimization of device-to-device (D2D) communications underlying a multi-cell massive multiple-input single-output (m-MISO) network, assuming that the channels are modeled with Rician fading. First, an analytical expression for the lower-bound of the ergodic capacity of a typical cellular user (CU) is derived with imperfect channel state information in the presence of D2D links' interference. Then, a closed-form approximate achievable SE expression for a typical D2D pair is derived considering Rician fading between D2D pairs. The asymptotic SE behavior is analyzed in strong line-of-sight (LOS) conditions for CU and D2D pairs. Also, simplified expressions are obtained for the special case of Rayleigh fading. Next, to optimize the total EE, a transmit data power allocation based on the derived rate expressions is formulated. Since the optimization problem has a non-linear and non-convex objective function, it is intractable to be solved straightforwardly. Therefore, we resort to utilizing an iterative algorithm relying on fractional programming. The numerical results show that a stronger LOS component (i.e., larger Rician K-factor) between a typical CU and its serving BS leads to a significant improvement in the system performance, while it has less effect on the D2D network.**

***Index Terms*—Device-to-device, fractional programming, multi-cell MISO, power control, Rician fading.**

I. Introduction

DEVICE-TO-DEVICE (D2D) communications has been proposed as a promising underlay coexistence with cellular networks due to compelling advantages such as offloading cellular traffic, providing better user experience, increasing the overall network spectral efficiency (SE), energy efficiency (EE), and extending the battery lifetime of user equipment [1], [2]. Initially, important features of D2D have been introduced in 3GPP LTE Release 12, and recently there is a general idea that it can be envisioned in future 6th generation of mobile networks (6G) [3] to establish high-speed data transmission while reducing the core network load [4]. D2D communications allows direct communication between neighboring mobile users, thus enhancing network throughput, reducing energy consumption and allowing the cellular network to serve more mobile users [5], [6].

There are two main operational schemes in inband D2D communications, namely, *overlaid (dedicated)* and *underlaid (reuse)* modes. In the *overlaid* mode, a portion of radio spectrum is dedicated to D2D pairs. Thus, there is no interference to the cellular users (CUs), albeit having inefficient resource utilization. However, in the *underlaid* mode, D2D pairs reuse the shared spectrum resources occupied by the CUs. Additionally, multiple D2D pairs can share the same resource; thus, there is inevitable interference from/to the cellular network [7]. Since the underlaid D2D communications exploits the same spectrum as CUs, the D2D users may have severe interference on the CUs, particularly in densely deployed networks. To overcome this issue, we can benefit from the advantages of massive multiple-input multiple-output (m-MIMO) systems, as they can improve the SE of both CU and D2D devices due to multiuser diversity gains. Consequently, the simultaneous operation of underlaid D2D communications with multiuser m-MIMO cellular networks at the same frequency band is one of the promising technologies in beyond 5G networks [3]. However, to efficiently leverage the available spectrum, proper resource allocation techniques [8], [9] need to be utilized to allocate the spectrum and optimize the transmit powers to further improve the overall system performance due to the existence of mutual interference signal [10]–[12].

The recent studies have considered various aspects of the coexistence of an underlaid D2D network and a single-cell m-MIMO cellular network in either uplink (UL) or downlink (DL) [13]–[20]. The work in [13] studied the optimization of transmit power with a maximization of D2D users' SE subject to rate constraints for cellular users in the UL of a single cell m-MIMO. A frequency-division duplexing m-MIMO system was considered in [14], where cascaded precoding is employed to reduce the limited feedback overhead. The authors investigate different D2D user cooperation schemes to improve the total sum-rate of the system. The authors in [15] investigated

Manuscript received 10 December 2021; revised 9 February 2022 and 14 March 2022; accepted 18 July 2022. Date of publication 21 July 2022; date of current version 15 February 2023. This work was supported in part by the Iran National Science Foundation (INSF) under Grant 96007127 and Grant 9701279. The editor coordinating the review of this article was C. Mavromoustakis. *(Corresponding author: Ramin Hashemi.)*

Ramin Hashemi was with the Department of Electrical Engineering, Amirkabir University of Technology, Tehran 15914, Iran. He is now with the Centre for Wireless Communications, University of Oulu, 90014 Oulu, Finland (e-mail: ramin.hashemi@oulu.fi).

Mohammad Kazemi was with the Department of Electrical Engineering, Amirkabir University of Technology, Tehran 15914, Iran. He is now with the Department of Electrical and Electronics Engineering, Bilkent University, 06800 Ankara, Turkey (e-mail: kazemi@ee.bilkent.edu.tr).

Abbas Mohammadi is with the Department of Electrical Engineering, Amirkabir University of Technology, Tehran 15914, Iran (e-mail: abm125@aut.ac.ir).

Digital Object Identifier 10.1109/TGCN.2022.3193071

the trade-off between SE and EE in D2D-enabled m-MIMO systems. They showed that coexistence of D2D and cellular networks are mainly beneficial in low densities of the D2D users. A pilot scheduling scheme was proposed in [16], where the D2D users partially reuse the orthogonal pilots of the CUs. It was shown that this scheme provides the same performance as a conventional underlaid D2D system while reducing the pilot overhead considerably. A distributive online learning algorithm was proposed in [17] for rate adaptation in scenarios where even the distribution of user signal-to-interference-plus-noise-ratios (SINR) is not known at the base station (BS). In order to mitigate the effect of pilot contamination when the D2D and CU users use the same set of orthogonal pilots, a pilot reuse scheme based on a graph coloring technique has been introduced in [18]. The work in [19] proposed a revised graph coloring-based pilot allocation algorithm with fast convergence for pilot contamination mitigation. An achievable rate analysis and optimization of underlaid D2D cell-free m-MIMO system involving finite resolution digital-to-analog converters were studied in [20], [21], assuming a Rayleigh fading channel model.

Multi-cell m-MIMO scenario is also studied in various works, e.g., in [22]–[27]. Closed-form expressions for the SE of D2D users and CUs employing a stochastic geometry approach were obtained in [22]. They also provided sufficient conditions to achieve a certain SE, as well as a spatially dynamic power control scheme that minimizes the cellular-to-D2D and D2D-to-cellular interference. The authors in [23] presented a statistical analysis of the achievable ergodic rate bounds for CUs in a multi-cell m-MIMO setup under least square and minimum mean-square-error (MMSE) channel estimation schemes. It is worth noting that the considered network does not incorporate D2D communications while the channel response of the associated users in a BS follow Rician fading. The uplink performance of a multi-cell m-MIMO system with underlaid D2D pairs was investigated in [24]. More precisely, asymptotic SE behavior of cellular and D2D pairs with perfect and imperfect channel state information (CSI) using orthogonal pilots without power control was analyzed. They showed that if a subset of interfering D2D users can be canceled in each transmission, the interference due to the underlaid D2D network can be overcome at the BS by increasing the number of antennas. The authors in [25] derived the SE expressions of both cellular CUs and D2D users assuming orthogonal pilots for channel estimation and employing maximal ratio combining (MRC) and zero-forcing (ZF) detection schemes in a multi-cell m-MIMO system with a Rayleigh fading channel. Moreover, two power allocation schemes were provided, one maximizing the minimum SE and the other maximizing the product of SINRs of all the users in the system. The study in [26] employed a pilot gray wolf prey (PGWO) algorithm for power control and pilot allocation in order to alleviate the pilot contamination problem in m-MIMO systems. A recent work [27] considered an incentive relaying scheme for single-antenna D2D and CU devices to collaboratively increase the overall throughput of the multi-cell network.

All the aforementioned studies have assumed a Rayleigh fading channel. However, due to short transmission distances, there is usually a line-of-sight (LOS) component in the channel response between D2D pairs or in the channels between serving BSs and their associated CUs. Although assuming a Rayleigh fading model simplifies the rate expressions, it is unrealistic in the underlaid D2D networks and can lead to inaccurate results, particularly since a strong LOS component affects the system performance considerably. Note that leveraging existing results of the Rayleigh fading model on the achievable rate of D2D pairs does not reflect the influence of such channels on the system performance. Therefore, analyzing the performance of cellular networks in terms of a more realistic and general channel distribution is of paramount importance. To this end, several studies have investigated the performance of multi-cell m-MIMO systems over a more general fading model such as Rician fading, however, without considering an underlaid D2D network [28]–[31]. In [28] the achievable rate of CUs in the UL and DL of a multi-cell m-MIMO system under Rician fading channel between BS and CUs was obtained in the presence of pilot contamination. It was also shown that although the closed-form expressions are obtained for the m-MIMO regime, they are accurate for the scenarios with fewer antennas at BS. The study in [29] investigated the uplink SE of linear MMSE estimation receivers considering two generalized fading models, namely $\kappa-\mu$ and $\eta-\mu$, which together encompass many practical fading models such as Rayleigh, Rician and Nakagami-m. The authors in [30] studied the probability of successful transmission and area spectral efficiency in a D2D-enabled traditional cellular network by stochastic geometry analysis. Also, they considered a mode selection as well as a centralized opportunistic access control scheme in order to minimize the cross-tier interference between cellular and D2D networks. The authors in [31] discussed an underlaid D2D multi-cell multi-channel system with Rician fading, however, with single-antenna base stations. Then, a multi-objective optimization approach was employed to maximize the closed-form expression for SE while minimizing the total transmit power of the D2D users. To best of our knowledge, the analysis of underlaid D2D-enabled multi-cell m-MISO systems over a Rician fading channel has not been considered yet. A concise comparison of the existing similar works is presented in Table I.

In this paper, we study the uplink of a D2D-enabled multi-cell m-MISO network over a Rician fading channel. The D2D devices operate on the *in-band* spectrum in a Rician multi-path fading as a general distribution compared with the Rayleigh fading. We consider MRC technique at the BSs to detect the transmitted signal of CUs under imperfect CSI. The channel coefficients are estimated by employing the MMSE estimation method using transmitted pilot signals. Furthermore, we present closed-form SE expressions for CUs and D2D devices. The main contributions are summarized as follows:

- A thorough analysis to incorporate Rician fading model in D2D-enabled communications is proposed. To this end, by assuming training-based CSI based on pilot transmission, we derive a lower-bound for the SE of CUs in a D2D communication underlying multi-cell massive multiple-input single-output (m-MISO) network using MRC where

TABLE I
CONCISE COMPARISON OF THE EXISTING WORKS

Ref.	System model	Channel model	SE analysis	Incorporating D2D	EE optimization
[13]	SIMO, UL	Rayleigh fading	✓	✓	–
[14]	Single-cell m-MIMO, DL	Rayleigh fading	–	✓	–
[15]	Single-cell multi-user MISO, DL	Rayleigh fading	✓	–	Only analysis
[16]	Single-cell multi-user SIMO, UL	Correlated Rayleigh fading	–	✓	–
[17]	Multi-cell multi-user MISO, DL	Rayleigh fading	✓	✓	–
[18]	Single-cell multi-user MISO, UL	Rayleigh fading (between D2D pairs)	✓	✓	–
[19]	Single-cell multi-user MISO*, UL	Rayleigh fading	✓	✓	–
[22]	Multi-cell MIMO, UL	Rayleigh fading	Stochastic geometry	✓	Only analysis
[23]	Multi-cell MIMO, UL	Rician fading	✓	–	–
[24]	Single-cell MIMO, UL	Rayleigh fading	✓	✓	–
[25], [26]	Multi-cell MIMO, UL	Rayleigh fading	✓	✓	–
[28]	Multi-cell multi-user MISO, UL	Rician fading	✓	–	–
[29–31]	Multi-cell multi-user SISO	Generalized [29] or Rician [30] fading	Stochastic geometry	✓	Only in [31]
Our work	Multi-cell multi-user MISO, UL with pilot re-use	Rician fading	✓	✓	✓

* D2D users are in SIMO mode, i.e., the receivers have multiple antennas.

the channel between a CU and its serving BS follows Rician distribution.

- We derive an approximate closed-form expression for ergodic capacity of D2D pairs where the channel between the D2D transmitters and their associated receivers is assumed to have a LOS path of which its power is the Rician fading parameter.
- We formulate an EE optimization framework by leveraging the obtained closed-form expressions on the SE. Then, employing an iterative algorithm based on fractional programming, we solve for the transmit powers of all devices.

The rest of the paper is organized as follows. In Section II, we study the network architecture. In Section III, we derive a lower-bound on SE of CUs assuming imperfect CSI at the BS. Moreover, we present a closed-form expression for the ergodic capacity of the D2D pairs. In Section IV, we formulate the EE optimization problem for determining the transmit power of devices and propose an iterative algorithm based on fractional programming to solve it. Finally, in Section V, the numerical results are presented, and Section VI concludes the paper.

Notations — Throughout this paper, the vectors are indicated by boldface letters and we use $\mathbf{X}^H$ and x^* to denote the conjugate transpose of $\mathbf{X}$ and conjugate of complex number x, respectively. Also, the operators $\mathbb{E}[\,\cdot\,]$ and $\mathbb{V}[\,\cdot\,]$ denote the statistical mean and variance operators, respectively. Moreover, a circularly symmetric complex Gaussian random vector $\mathbf{x}$ with zero mean and covariance matrix $\mathbf{B}$ is shown as $\mathbf{x} \sim \mathcal{CN}(\mathbf{0}_M, \mathbf{B})$, where $\mathbf{0}_M$ is an all-zero vector of length M.

II. SYSTEM MODEL

Consider the uplink of a multi-cell m-MISO cellular system with B cells, surrounded by L underlaid single-antenna D2D pairs. In each cell, there are a BS equipped with M antennas and K single-antenna CUs. The transmission is done in two phases. In the first phase, the BSs estimate their users' channel coefficients using uplink pilot training. In the second phase, the users send their data to their corresponding BS, and the BSs perform data detection using the estimated channel coefficients. The network architecture is depicted in Fig. 1. Note that the D2D devices are connected to the cloud

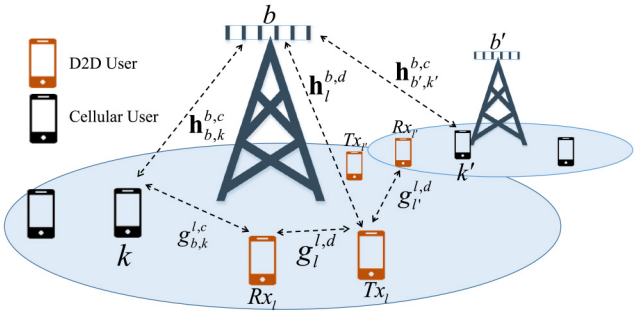

Fig. 1. Network architecture.

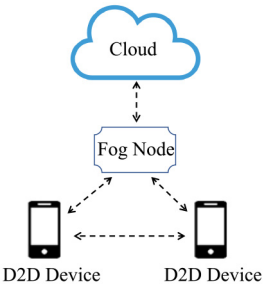

Fig. 2. A general scheme for the fog platform.

through fog nodes, which can be femtocell BSs or D2D devices themselves helping with the communication [32]. The general scheme of this fog platform is depicted in Fig. 2. The assumed architecture in this paper, as described in Figs. 1 and 2, has numerous applications in 5G and beyond systems ranging from smart homes to post-disaster communication networks. As an example, in unlicensed communications in beyond 5G systems, a common spectrum is going to be shared between the cellular network and other unlicensed ones such as machine-to-machine systems which rely on the D2D communications [33]. According to the system model in Fig. 1, the channel vector between the b-th BS and the k-th CU in the b'-th BS is expressed by [34]

$$\mathbf{h}_{b',k}^{b,c} = \begin{cases} \sqrt{\frac{K_{bk}}{K_{bk}+1}}\overline{\mathbf{h}}_{b,k}^{b,c} + \sqrt{\frac{1}{K_{bk}+1}}\mathbf{h}_{b,k,\mathrm{NLOS}}^{b,c}, & \text{if } \ b' = b \\ \mathbf{h}_{b',k,\mathrm{NLOS}}^{b,c}, & \text{if } b' \neq b \end{cases} \tag{1}$$

TABLE II
PARAMETERS AND NOTATIONS USED IN THE PAPER

Notation	Description	Notation	Description
CU_k^b	k-th CU in b-th cell	$\mathrm{D2D}_l$	l-th D2D pair
$\mathbf{h}_{b,k}^{b',c}$	Channel vector between CU_k^b and b'-th BS	$\mathbf{h}_l^{b,d}$	Channel vector between $\mathrm{D2D}_l$ and b-th BS
$g_{l'}^{l,d}$	Channel coefficient between Tx of $\mathrm{D2D}_l$ and Rx of $\mathrm{D2D}_{l'}$	$g_{b,k}^{l,c}$	Channel coefficient between Rx of $\mathrm{D2D}_l$ and CU_k^b
$p_{b,k}^c$	Transmit power of CU_k^b	p_l^d	Transmit power of $\mathrm{D2D}_l$
$p_{b,k}^{p,c}$	Transmit pilot power of CU_k^b	$p_l^{p,d}$	Transmit pilot power of $\mathrm{D2D}_l$
$s_{b,k}^c$	Data symbol transmitted from CU_k^b	s_l^d	Data symbol transmitted from $\mathrm{D2D}_l$
K_{bk}	Rician K-factor of CU_k^b	K_l	Rician K-factor of $\mathrm{D2D}_l$
$\beta_{b,k}^{b',c}$	Large-scale coefficient between CU_k^b and b'-th BS	$\beta_l^{b,c}$	Large-scale coefficient between $\mathrm{D2D}_l$ and b-th BS
$\beta_{l'}^{l,d}$	Large-scale coefficient $\mathrm{D2D}_l$ and $\mathrm{D2D}_{l'}$	λ	Wavelength
$\boldsymbol{\phi}_l^d$	Pilot sequences assigned to $\mathrm{D2D}_l$	$\boldsymbol{\phi}_i^c$	Pilot sequences assigned to i-th CU
$\gamma_{b,k}^{b,c}$	Normalized norm squared of channel estimate $\hat{\mathbf{h}}_{b,k}^{b,c}$	$\gamma_l^{b,d}$	Normalized norm squared of channel estimate $\hat{\mathbf{h}}_l^{b,d}$
$\gamma_{l'}^{l,d}$	Normalized norm squared of channel estimate $\hat{g}_{l'}^{l,d}$	N_i	The indices of D2D pairs that are using $\boldsymbol{\phi}_i^d$
$p_l^{d,ci}$	Circuit power consumption of $\mathrm{D2D}_l$	$p_{b,k}^{c,ci}$	Circuit power consumption of the CU_k^b
τ	Length of pilot sequence	$\theta_{b,k}$	Angle of arrival between BS b and CU k
N	Number of pilot sequences for D2D pairs	L	Total number of D2D pairs

where K_{bk}, and $\overline{\mathbf{h}}_{b,k}^{b,c} \in \mathbb{C}^{M\times 1}$ are the Rician K-factor, and the LOS component of the channel vector of the k-th CU in the b-th cell, respectively. Also, $\mathbf{h}_{b',k,\mathrm{NLOS}}^{b,c} \sim \mathcal{CN}(\mathbf{0}_M, \beta_{b',k}^{b,c}\mathbf{I}_M)$ is the non-line-of-sight (NLOS) component $\forall b, b'$, where $\mathbf{I}_K$ is the $K \times K$ identity matrix. Note that this model is a composite fading model, taking into account the effects of both small-scale fading through $\mathbf{h}_{b,k,\mathrm{NLOS}}^{b,c}$, and large-scale fading through $\overline{\mathbf{h}}_{b,k}^{b,c}$ and $\beta_{b,k}^{b,c}$, which is simplified to a Rayleigh fading model when the Rician K-factor is set to zero. In (1), $\overline{\mathbf{h}}_{b,k}^{b,c} \in \mathbb{C}^{M\times 1}$ is modeled as [35]

$$\left[\overline{\mathbf{h}}_{b,k}^{b,c}\right]_m = \sqrt{\beta_{b,k}^{b,c}} e^{\frac{-j(m-1)2\pi}{\lambda}\sin(\theta_{bk})}, \tag{2}$$

where λ is the wavelength and $\theta_{bk} \in [0, 2\pi)$ is the angle of arrival. We assume that the LOS components are known at the BSs. In addition, the channel response between the transmitter of D2D pair l and the BS is denoted by $\mathbf{h}_l^{b,d} \sim \mathcal{CN}(\mathbf{0}_M, \beta_l^{b,d}\mathbf{I}_M)$ where $\beta_l^{b,d}$ is the large-scale fading coefficient.

The parameters and notations that are used in the paper are summarized in Table II.

A. Pilot Transmission and Channel Estimation

1) Cellular Users: It is assumed that the channel coefficients are estimated at each coherence time interval prior to data transmission. Therefore, CUs and D2D pairs transmit pilot sequences of length τ for channel estimation at the BS. Let us assume that the set of CUs in a BS use orthogonal pilot sequences, i.e., they exploit K orthogonal pilot sequences. In addition, $N \leq L$ sequences are assigned to D2D pairs. Hence, the total number of pilot sequences is $\tau = N + K$. During the uplink channel training, the received pilot signal $\mathbf{Y}_b^{\mathrm{training}} \in \mathbb{C}^{M\times\tau}$ from cellular users and D2D transmitters at the b-th BS can be written as

$$\mathbf{Y}_b^{\mathrm{training}} = \underbrace{\sum_{k=1}^{K}\sum_{b'=1}^{B}\sqrt{\tau p_{b',c}^{p,c}(K_{b'k}+1)}\mathbf{h}_{b',k}^{b,c}(\boldsymbol{\phi}_k^c)^H}_{\text{Term1 : CUs pilot signal}} + \underbrace{\sum_{i=1}^{N}\sum_{l\in N_i}\sqrt{\tau p^{p,d}}\mathbf{h}_l^{b,d}(\boldsymbol{\phi}_i^d)^H}_{\text{Term2 : D2D pairs pilot signal}} + \mathbf{W}_b, \tag{3}$$

where $\boldsymbol{\phi}_k^c$ is the pilot sequence assigned to the k-th CU, N_i denotes the indices of D2D pairs that are using the D2D dedicated pilot sequence $\boldsymbol{\phi}_i^d$, and $\mathbf{W}_b$ is the additive circularly symmetric complex Gaussian noise at the b-th BS with zero mean vector and identity covariance matrix $\mathbf{I}_M$; i.e., $\mathbf{W}_b \sim \mathcal{CN}(\mathbf{0}_{M\times\tau}, \mathbf{I}_M)$. We assume that the assigned pilot signals to the D2D pairs and CUs are orthogonal, and that the same set of pilot are reused in each cell, i.e., $(\boldsymbol{\phi}_k^c)^H\boldsymbol{\phi}_k^c = 1$, $\forall k \in \mathcal{K}$, $(\boldsymbol{\phi}_{k'}^c)^H\boldsymbol{\phi}_k^c = 0$ for $k' \neq k$, and $(\boldsymbol{\phi}_i^d)^H\boldsymbol{\phi}_k^c = 0$, $\forall i \in \mathcal{L}$, $\forall k \in \mathcal{K}$, where $\mathcal{K}$ and $\mathcal{L}$ are sets of all CUs in each cell and all D2D pairs. In other words, due to orthogonality of the pilot sequences for CU and D2D devices, the expression of Term2 in (3) is removed by multiplying the received pilot signal with the known CU codebook $\boldsymbol{\Phi}^c$ to extract the CU channel coefficients.

Furthermore, the BS b despreads the received pilot signal from CUs as given by

$$\begin{aligned}\mathbf{Y}_b^{\mathrm{training}}\boldsymbol{\Phi}^c &= \sum_{k=1}^{K}\sum_{b'=1}^{B}\sqrt{\tau p_{b',k}^{p,c}(K_{b'k}+1)}\mathbf{h}_{b',k}^{b,c}(\boldsymbol{\phi}_k^c)^H\boldsymbol{\Phi}^c \\ &\quad + \mathbf{W}^b\boldsymbol{\Phi}^c \\ &= \sqrt{\tau p_{b,k}^{p,c}(K_{bk}+1)}\left(\sqrt{\frac{K_{bk}}{K_{bk}+1}}\overline{\mathbf{h}}_{b,k}^{b,c} \right. \\ &\quad \left. + \sqrt{\frac{1}{K_{bk}+1}}\mathbf{h}_{b,k,\mathrm{NLOS}}^{b,c}\right)\end{aligned}$$

$$+\sum_{b'=1,b'\neq b}^{B}\sqrt{\tau p_{b',k}^{p,c}(K_{b'k}+1)}\mathbf{h}_{b',k,\mathrm{NLOS}}^{b,c}(\boldsymbol{\phi}_k^c)^H\boldsymbol{\Phi}^c +\mathbf{W}^b\boldsymbol{\Phi}^c, \quad (4)$$

where $\boldsymbol{\Phi}^c$ is the set of all CU pilot sequences in each cell, i.e., $\boldsymbol{\Phi}^c=[\boldsymbol{\phi}_1^c,\boldsymbol{\phi}_2^c,\ldots,\boldsymbol{\phi}_K^c]$.

Since the LOS components are assumed to be known at the BS, the other NLOS channels' estimation can be performed by subtracting the LOS signal from (4) that is simplified as

$$\overline{\mathbf{Y}_b^{\text{training}}\boldsymbol{\Phi}^c}=\sqrt{\tau p_{b,k}^{p,c}}\mathbf{h}_{b,k,\mathrm{NLOS}}^{b,c} +\sum_{\substack{b'=1,\\ b'\neq b}}^{B}\sqrt{\tau p_{b',c}^{b,c}(K_{b'k}+1)}\mathbf{h}_{b',k,\mathrm{NLOS}}^{b,c}(\boldsymbol{\phi}_k^c)^H\boldsymbol{\Phi}^c + \mathbf{W}^b\boldsymbol{\Phi}^c, \quad (5)$$

where $\overline{\mathbf{Y}_b^{\text{training}}\phi^c}$ is $\mathbf{Y}_b^{\text{training}}\phi^c$ without the presence of the LOS component.

Proposition 1: The estimated NLOS channel coefficient $\hat{\mathrm{h}}_{b,k,\mathrm{NLOS}}^{b,c}$ can be written as

$$\hat{\mathrm{h}}_{b,k,\mathrm{NLOS}}^{b,c}=\chi\left(\mathrm{h}_{b,k,\mathrm{NLOS}}^{b,c}+\sum_{b'=1,b'\neq b}^{B}\times\sqrt{\frac{\tau p_{b',k}^{p,c}(K_{b'k}+1)}{\tau p_{b,k}^{p,c}}}\mathrm{h}_{b',k,\mathrm{NLOS}}^{b,c}+\frac{1}{\sqrt{\tau p_{b,k}^{p,c}}}\tilde{\mathrm{n}}_{bk}\right), \quad (6)$$

where $\tilde{\mathrm{n}}_{bk}$ is the circularly symmetric complex Gaussian noise $\mathcal{CN}(0_M,\mathrm{I}_M)$ and

$$\chi=\frac{\tau p_{b,k}^{p,c}\beta_{b,k}^{b,c}}{\tau p_{b,k}^{p,c}\beta_{b,k}^{b,c}+\sum_{b'=1,b'\neq b}^{B}\tau p_{b',c}^{b,c}(K_{b'k}+1)\beta_{b',k}^{b,c}+1}. \quad (7)$$

Proof: Please refer to Appendix A. ∎

Note that the terms in (5) have been treated as an uncorrelated noise during MMSE procedure except for the intended term that is being estimated. Also, as noted earlier, we assumed that the LOS components of the channel are a priori known at the BS. Thus, the estimation of the CSI will be only performed for NLOS component of the channel response. Consequently, denoting $\hat{\mathbf{h}}_{b',k,\mathrm{NLOS}}^{b,c}$ as the estimator of $\mathbf{h}_{b',k,\mathrm{NLOS}}^{b,c}$, and utilizing the Rician fading distribution with parameter $K_{b,k}$ in (1), the final estimated channel coefficient can be written as [23]

$$\hat{\mathbf{h}}_{b,k}^{b,c}=\sqrt{\frac{K_{bk}}{K_{bk}+1}}\overline{\mathbf{h}}_{b,k}^{b,c}+\sqrt{\frac{1}{K_{bk}+1}}\hat{\mathbf{h}}_{b,k,\mathrm{NLOS}}^{b,c}. \quad (8)$$

Similarly, to extract the D2D pairs' channel coefficients, the D2D codebook matrix $\boldsymbol{\Phi}^d$ is multiplied by the received pilot signal resulting in Term1 in (3) being omitted in this case. First, considering pilot signal processing for D2D pairs, despreading of the received signal at the b-th BS yields

$$\mathbf{Y}_b^{\text{training}}\boldsymbol{\Phi}^d=\sum_{i=1}^{N}\sum_{l\in N_i}\sqrt{\tau p_l^{p,d}}\mathbf{h}_l^{b,d}(\boldsymbol{\phi}_i^d)^H\boldsymbol{\Phi}^d+\mathbf{W}\boldsymbol{\Phi}^d, \quad (9)$$

where $\boldsymbol{\Phi}^d$ is the set of all D2D pilot sequences, i.e., $\boldsymbol{\Phi}^d=[\boldsymbol{\phi}_1^d,\boldsymbol{\phi}_2^d,\ldots,\boldsymbol{\phi}_L^d]$. To obtain an estimate for the channel coefficients vector $\mathbf{h}_l^{b,d}$ from the received pilot training signal in (9), the MMSE scheme is employed. Since it is similar to the estimation of CU channel coefficients in Proposition 1, we omit the details of mathematical manipulations and report the final expression as

$$\hat{\mathbf{h}}_l^{b,d}=\chi'\left(\mathbf{h}_l^{b,d}+\sum_{i=1}^{N}\sum_{l'\in N_i,l'\neq l}\sqrt{\tau p_{l'}^{p,d}}\mathbf{h}_{l'}^{b,d}+\tilde{\mathbf{n}}_l\right), \quad (10)$$

where $\chi'=\frac{\tau p_l^{p,d}\beta_l^{b,d}}{1+\sum_{l'\in N_i}\tau p_{l'}^{p,d}\beta_{l'}^{b,d}}$ and $\tilde{\mathbf{n}}_l\sim\mathcal{CN}(\mathbf{0}_M,\mathbf{I}_M)$. Finally, the estimation variances are computed straightforwardly (in a similar manner as in [36]) as

$$\mathbb{E}\left[\left\|\hat{\mathbf{h}}_l^{b,d}\right\|^2\right]=\gamma_l^{b,d}M, \quad (11)$$

$$\mathbb{E}\left[\left\|\hat{\mathbf{h}}_{b,k,\mathrm{NLOS}}^{b,c}\right\|^2\right]=\gamma_{b,k}^{b,c}M, \quad (12)$$

where

$$\gamma_l^{b,d}=\frac{\tau p_l^{p,d}(\beta_l^{b,d})^2M}{1+\sum_{l'\in N_i}\tau p_{l'}^{p,d}\beta_{l'}^{b,d}}, \quad (13)$$

$$\gamma_{b,k}^{b,c}=\frac{\tau p_{b,k}^{p,c}\left(\beta_{b,k}^{b,c}\right)^2M}{1+\tau p_{b,k}^{p,c}\beta_{b,k}^{b,c}+\sum_{b'=1,b'\neq b}^{B}\tau p_{b',k}^{p,c}(K_{b'k}+1)\beta_{b',k}^{b,c}}. \quad (14)$$

2) D2D Users: Since the assigned pilot signals to the D2D pairs and CUs are orthogonal to each other, the received signal at the l-th D2D receiver in the training phase after despreading for the D2D channel coefficient (i.e., multiplying with $\boldsymbol{\Phi}^d$) is given by

$$y_{\text{training}}^{l,d}=\sum_{l''\in N_i}\sqrt{\tau p_{l''}^{p,d}}g_{l''}^{l,d}+w_l^d, \quad (15)$$

which is used in estimating $g_l^{l,d}$ (knowing $w_l^d\sim\mathcal{CN}(0,1)$).

On the other hand, the received signal at the l-th D2D receiver in the training phase after despreading for the channel coefficients between the CUs and the D2D receivers (i.e., multiplying with $\boldsymbol{\Phi}^c$) can be written as

$$y_{b,k,\text{training}}^{l,c}=\sum_{b'=1}^{B}\sqrt{\tau p_{b',k}^{p,c}}g_{b',k}^{l,c}+w_l^c, \quad (16)$$

which is used in estimating $g_{b,k}^{l,c}$ (knowing $w_l^c\sim\mathcal{CN}(0,1)$). In addition, we suppose the following model for the channel between D2D devices

$$\hat{g}_{l'}^{l,d}=\begin{cases}\sqrt{\frac{K_{l'}}{(K_{l'}+1)}}\overline{g}_l^{l,d}+\sqrt{\frac{1}{(K_{l'}+1)}}\hat{g}_{l,\mathrm{NLOS}}^{l,d}, & \text{if } l'=l\\ \hat{g}_{l',\mathrm{NLOS}}^{l,d} & \text{if } l'\neq l\end{cases} \quad (17)$$

which is similar to the channel model between the CUs and the BS, except that here the LOS component is independent of angle of arrival since D2D users employ omni-directional

antennas. We assume that the LOS component of $g_l^{l,d}$ is a priori known at the D2D receiver, hence, the channel estimation is only conducted for the NLOS part. Similar to the previous section, using (15) and (17) and employing the MMSE estimation technique $\hat{g}_{l,\text{NLOS}}^{l,d}$ can be estimated as [37]

$$\hat{g}_{l,\text{NLOS}}^{l,d} = \chi'' \left(\sqrt{\frac{\tau p_l^{p,d}}{K_l+1}} g_{l,\text{NLOS}}^{l,d} + \sum_{\substack{l'' \in N_i \\ l'' \neq l}} \sqrt{\tau p_{l''}^{p,d}} g_{l'',\text{NLOS}}^{l,d} + \tilde{n}_l^d \right), \quad (18)$$

where $\tilde{n}_l^d \sim \mathcal{CN}(0,1)$ and

$$\chi'' = \frac{\sqrt{\frac{\tau p_l^{p,d}}{K_l+1}} \beta_l^{l,d}}{1 + \frac{\tau p_l^{p,d}}{K_l+1} \beta_l^{l,d} + \sum_{l'' \in N_i, l'' \neq l} \tau p_{l''}^{p,d} \beta_{l''}^{l,d}}. \quad (19)$$

Therefore, the channel estimation variance will be

$$\mathbb{E}\left[\left\| \hat{g}_{l,\text{NLOS}}^{l,d} \right\|^2 \right] = \gamma_l^{l,d} = \frac{\frac{\tau p_l^{p,d}}{K_l+1} \left(\beta_l^{l,d} \right)^2}{1 + \frac{\tau p_l^{p,d}}{K_l+1} \beta_l^{l,d} + \sum_{l'' \in N_i, l'' \neq l} \tau p_{l''}^{p,d} \beta_{l''}^{l,d}}.$$

In the next section, closed-form expressions for the performance of the CUs and the D2D pairs will be studied in detail.

III. Capacity Analysis

A. Cellular Network

The CUs and the D2D pairs transmit their data signals intended for their associated BS and D2D receivers, respectively. Accordingly, the received data signal vector $\mathbf{y}_b^c \in \mathbb{C}^{M \times 1}$ at the b-th BS can be written as

$$\mathbf{y}_b^c = \overbrace{\sqrt{p_{b,k}^c} \mathbf{h}_{b,k}^{b,c} s_{b,k}^c}^{\text{desired signal}} + \overbrace{\sum_{k'=1, k' \neq k}^{K} \sqrt{p_{b,k'}^c} \mathbf{h}_{b,k'}^{b,c} s_{b,k'}^c}^{\text{intra-cell interference}} + \underbrace{\sum_{\substack{b'=1, \\ b' \neq b}}^{B} \sum_{\substack{k'=1, \\ k' \neq k}}^{K} \sqrt{p_{b',k'}^c} \mathbf{h}_{b',k'}^{b,c} s_{b',k'}^c}_{\text{inter-cell interference}} + \underbrace{\sum_{l=1}^{L} \sqrt{p_l^d} \mathbf{h}_l^{b,d} s_l^d}_{\text{D2D interference}} + \mathbf{w}_b, \quad (20)$$

where $s_{b,k}^c$ and s_l^d are the data symbols transmitted from the k-th CU in the b-th BS and the l-th D2D transmitter, respectively, and $\mathbf{w}_b$ is the additive circularly symmetric complex Gaussian noise at the b-th BS with $\mathbf{w}_b \sim \mathcal{CN}(\mathbf{0}_M, \mathbf{I}_M)$. Note that superscripts c and d are employed to distinguish the parameters associated with the CUs and the D2D pairs, respectively. After estimating the channel coefficients in the uplink channel training phase, the BS employs the MRC technique to detect the users' data. In the following theorem, we propose a lower-bound on the SE of a typical CU.

Theorem 1: By employing the MRC data detection at the BS, the spectral efficiency of the k-th CU in the b-th cell $R_k^{b,c}$ can be lower-bounded as follows.

$$R_k^{b,c} \geq \log_2\left(1 + \text{SINR}_k^{b,c}\right), \quad (21)$$

where

$$\text{SINR}_k^{b,c} = \frac{p_{b,k}^c M^2 \left(\beta_{b,k}^{b,c}\right)^2}{\text{I}_1 + \text{I}_2 + \text{I}_3}, \quad (22)$$

with

$$\text{I}_1 = \sum_{b'=1}^{B} \sum_{k'=1}^{K} p_{b',k'}^c \mathcal{I}_{k',b'}, \quad \text{I}_2 = \sum_{l=1}^{L} p_l^d \mathcal{I}_l, \quad (23)$$

$$\text{I}_3 = M \beta_{b,k}^{b,c} + M \frac{\sum_{b'=1, b' \neq b}^{B} \tau p_{b',k}^{p,c} (K_{b'k}+1) \beta_{b',k}^{b,c} + 1}{\tau p_{b,k}^{p,c} (K_{bk}+1)}, \quad (24)$$

where $\mathcal{I}_{k',b'}$ and $\mathcal{I}_l$ are given in (25)–(28)

$$\mathcal{I}_{k',b}^{k' \neq k} = \beta_{b,k}^{b,c} \beta_{b,k'}^{b,c} \frac{K_{bk} K_{bk'} \phi_{kk'}^2 + M(K_{bk} + K_{bk'}) + M}{(K_{bk'}+1)(K_{bk}+1)} + M \beta_{b,k}^{b,c} \frac{\sum_{b'=1, b' \neq b}^{B} \tau p_{b',k}^{p,c} (K_{b'k}+1) \beta_{b,k'}^{b,c} + 1}{\tau p_{b,k}^{p,c} (K_{bk}+1)}, \quad (25)$$

$$\mathcal{I}_{k,b'}^{b' \neq b} = M^2 \left(\beta_{b',k}^{b,c}\right)^2 \frac{\tau p_{b',k}^{p,c} (K_{b'k}+1)}{\tau p_{b,k}^{p,c} (K_{bk}+1)} + M \beta_{b,k}^{b,c} \beta_{b',k}^{b,c} + M \beta_{b',k}^{b,c} \frac{\sum_{b''=1, b'' \neq b}^{B} \tau p_{b'',k}^{p,c} (K_{b''k}+1) \beta_{b'',k}^{b,c} + 1}{\tau p_{b,k}^{p,c} (K_{bk}+1)}, \quad (26)$$

$$\mathcal{I}_{k',b'}^{k' \neq k, b' \neq b} = M \beta_{b',k'}^{b,c} \beta_{b,k}^{b,c} + M \beta_{b',k'}^{b,c} \frac{\sum_{b''=1, b'' \neq b}^{B} \tau p_{b'',k}^{p,c} (K_{b''k}+1) \beta_{b'',k}^{b,c} + 1}{\tau p_{b,k}^{p,c} (K_{bk}+1)}, \quad (27)$$

$$\mathcal{I}_l = M \beta_l^{b,d} \beta_{b,k}^{b,c} + M \beta_l^{b,d} \frac{\sum_{b'=1, b' \neq b}^{B} \tau p_{b',k}^{p,c} (K_{b'k}+1) \beta_{b',k}^{b,c} + 1}{\tau p_{b,k}^{p,c} (K_{bk}+1)}, \quad (28)$$

where $\phi_{kk'} = \frac{\sin(0.5M\pi(\sin\theta_{bk} - \sin\theta_{bk'}))}{\sin(0.5\pi(\sin\theta_{bk} - \sin\theta_{bk'}))}$.

Proof: The proof is provided in Appendix B. ■

B. D2D Network

In this section, we investigate an approximate expression for the capacity of the D2D receivers given this background. Simultaneous with the cellular network, the D2D transmitters send their data and channel training pilot sequences in the first and second phases, respectively. Similar to the previous

subsection, the received signal at the l-th D2D receiver, y_l^d, can be expressed as

$$y_l^d = \overbrace{\sqrt{p_l^d}\, g_l^{l,d}}^{\text{desired signal}} + \overbrace{\sum_{b=1}^{B}\sum_{k=1}^{K}\sqrt{p_{b,k}^c}\, g_{b,k}^{l,c}}^{\text{cellular users interference}} + \overbrace{\sum_{l'=1,l'\neq l}^{L}\sqrt{p_{l'}^d}\, g_{l'}^{l,d}}^{\text{D2D users interference}} + w_l, \tag{29}$$

where $w_l \sim \mathcal{CN}(0,1)$ is the Gaussian noise. In this study, we assume that the D2D receivers have the following CSI knowledge throughout data detection [25]

$$\Omega = \left\{ \hat{g}_{l',\text{NLOS}}^{l,d} \text{ for } \forall\ l' \in \mathcal{L}, \hat{g}_{b,k}^{l,c} \text{ for } \forall\ k \in \mathcal{K},\ \forall b \in \mathcal{B} \right\}, \tag{30}$$

where $\mathcal{B}$ is the set of all BSs. In other words, the receivers do not have a direct access to the channel estimates, and only a side information denoted by Ω is available.

After acquiring the channel estimates of D2D pairs, a closed-form expression for the approximation of ergodic capacity of the D2D pairs can be analytically derived as follows:

Theorem 2: The ergodic capacity of the l-th D2D pair can be approximated as

$$C_l^d \approx \log_2\left(1 + \text{SINR}_l^d\right), \tag{31}$$

with

$$\text{SINR}_l^d = \frac{\frac{p_l^d}{K_l+1}\left(K_l\beta_l^{l,d} + \gamma_l^{l,d}\right)}{\frac{p_l^d\left(\beta_l^{l,d} - \gamma_l^{l,d}\right)}{K_l+1} + \sum_{b=1}^{B}\sum_{k=1}^{K} p_{b,k}^c \beta_{l,c}^{b,k} + \sum_{l'=1,l'\neq l}^{L} p_{l'}^d \beta_{l'}^{l,d} + 1}. \tag{32}$$

Proof: The proof is provided in Appendix C. ∎

Corollary 1: When only the LOS component is present in D2D communications (i.e., $K_l \to \infty$), the approximate ergodic capacity of the l-th D2D pair can be obtained as

$$\lim_{K_l\to\infty} \tilde{C}_l^d = \log_2\left(1 + \frac{p_l^d \beta_l^{l,d}}{\sum_{b=1}^{B}\sum_{k=1}^{K} p_{b,k}^c \beta_{l,c}^{b,k} + \sum_{l'=1,l'\neq l}^{L} p_{l'}^d \beta_{l'}^{l,d} + 1}\right). \tag{33}$$

Proof: The result is obtained by letting K_l in (31) go to infinity. ∎

IV. Energy Efficiency Optimization

One of the key performance metrics in cellular networks is the relative energy efficiency measured as bits/Hz/Joule, particularly in D2D-enabled cellular networks. The relative EE is defined as the ratio of the total sum-rate of the system (cellular and D2D networks) and the total consumed power, i.e.,

$$\text{EE} = \frac{\sum_{b=1}^{B}\sum_{k=1}^{K} R_k^{b,c} + \sum_{l=1}^{L} \tilde{C}_l^d}{\sum_{b=1}^{B}\sum_{k=1}^{K}\left(p_{b,k}^c + p_{b,k}^{c,ci}\right) + \sum_{l=1}^{L}\left(p_l^d + p_l^{d,ci}\right)}, \tag{34}$$

where $p_l^{d,ci}$ and $p_{b,k}^{c,ci}$ represent the circuit power consumption of the l-th D2D transmitter and the k-th CU in the b-th cell, respectively.

In order to optimize the EE, we formulate an optimization framework which takes EE as the objective function as follows

$$\mathbf{P1}: \max_{\mathbf{p}^c,\mathbf{p}^d} \quad \text{EE}$$
$$\text{s.t.} \quad 0 \le p_{b,k}^c \le P_{b,k}^{\max}, \quad \forall k \in \mathcal{K}, \tag{35a}$$
$$0 \le p_l^d \le P_l^{\max}, \quad \forall l \in \mathcal{L}, \tag{35b}$$

where $\mathbf{p}^c$ contains $p_{b,k}^c$ for $\forall k \in \mathcal{K}, b \in \mathcal{B}$ and $\mathbf{p}^d$ contains p_l^d for $\forall l \in \mathcal{L}$. The maximum transmit power of CUs and D2D devices are denoted as $P_{b,k}^{\max}$ and $P_l^{\max}$, respectively. **P1** is a non-convex optimization problem, which needs high-complexity algorithms to reach a global optimal solution. Therefore, we resort to an alternative algorithm that achieves a sub-optimal result.

To begin with solving **P1** sub-optimally, consider the following tight lower-bound on the SE [38]

$$\ln(1 + \text{SINR}) \ge \eta \ln(\text{SINR}) + \zeta, \tag{36}$$

where $\ln(\cdot)$ denotes the natural logarithm and

$$\eta = \frac{\overline{\text{SINR}}}{\overline{\text{SINR}} + 1}, \tag{37a}$$
$$\zeta = \ln(1 + \overline{\text{SINR}}) - \eta \ln(\overline{\text{SINR}}), \tag{37b}$$

where $\overline{\text{SINR}}$ is the mean value of SINR. Using approximation (36) and with change of variables $\mathbf{p}^c = \exp(\tilde{\mathbf{p}}^c)$ and $\mathbf{p}^d = \exp(\tilde{\mathbf{p}}^d)$, **P1** is converted to the following optimization problem

$$\mathbf{P1.1}: \max_{\tilde{\mathbf{p}}^c,\tilde{\mathbf{p}}^d} \frac{\text{A}(\tilde{\mathbf{p}}^c,\tilde{\mathbf{p}}^d)}{\text{B}(\tilde{\mathbf{p}}^c,\tilde{\mathbf{p}}^d)}$$
$$\text{s.t.} \quad \tilde{p}_k^{b,c} \le \ln\left(P_{b,k}^{\max}\right), \quad \forall b \in \mathcal{B}, \forall k \in \mathcal{K}, \tag{38a}$$
$$\tilde{p}_l^d \le \ln(P_k^{\max}), \quad \forall l \in \mathcal{L}. \tag{38b}$$

where $\text{A}(\tilde{\mathbf{p}}^c,\tilde{\mathbf{p}}^d)$ and $\text{B}(\tilde{\mathbf{p}}^c,\tilde{\mathbf{p}}^d)$ are defined as

$$\text{A}\left(\tilde{\mathbf{p}}^c,\tilde{\mathbf{p}}^d\right) = \sum_{b=1}^{B}\sum_{k=1}^{K}\left(\eta_{b,k}^c \ln\left(\tilde{\text{SINR}}_k^{b,c}\left(\tilde{\mathbf{p}}^c,\tilde{\mathbf{p}}^d\right)\right) + \zeta_{b,k}^c\right) + \sum_{l=1}^{L}\left(\eta_l^d \ln\left(\tilde{\text{SINR}}_l^d\left(\tilde{\mathbf{p}}^c,\tilde{\mathbf{p}}^d\right)\right) + \zeta_l^d\right), \tag{39}$$

$$\text{B}\left(\tilde{\mathbf{p}}^c,\tilde{\mathbf{p}}^d\right) = \sum_{b=1}^{B}\sum_{k=1}^{K} e^{\tilde{p}_{b,k}^c} + \sum_{l=1}^{L} e^{\tilde{p}_l^d} + \sum_{b=1}^{B}\sum_{k=1}^{K} p_{b,k}^{c,ci} + \sum_{l=1}^{L} p_l^{d,ci}. \tag{40}$$

It can be easily proved that $\text{A}(\tilde{\mathbf{p}}^c,\tilde{\mathbf{p}}^d)$ and $\text{B}(\tilde{\mathbf{p}}^c,\tilde{\mathbf{p}}^d)$ are concave and convex functions, respectively; however, their ratio as the objective function makes the problem a non-convex fractional programming which is complex to solve. In order to tackle this issue, we employ *quadratic transformation* in [39]. The authors expressed four conditions on the transformed

optimization problem that should be satisfied, which are established by applying $\mathsf{f}(\cdot) = 2y\sqrt{\mathsf{N}} - y^2\mathsf{D}$ to a fractional objective function where N and D are the nominator and the denominator, respectively. Also, y is an auxiliary variable in $\mathbb{R}$, which is updated iteratively. By incorporating the transformation $\mathsf{f}(\cdot)$ on the **P1.1**, the objective function can be rewritten as

$$\mathrm{g}\Big(\tilde{\mathbf{p}}^c, \tilde{\mathbf{p}}^d, y\Big) = 2y\sqrt{\mathrm{A}\big(\tilde{\mathbf{p}}^c, \tilde{\mathbf{p}}^d\big)} - y^2\,\mathrm{B}\Big(\tilde{\mathbf{p}}^c, \tilde{\mathbf{p}}^d\Big), \quad (41)$$

where y is an auxiliary variable in $\mathbb{R}$. Therefore, the EE optimization **P1.1** is converted to

$$\mathbf{P1.2}: \max_{\tilde{\mathbf{p}}^c, \tilde{\mathbf{p}}^d, y} \quad \mathrm{g}\Big(\tilde{\mathbf{p}}^c, \tilde{\mathbf{p}}^d, y\Big) \quad (42)$$

$$\mathbf{s.t.} \quad \tilde{p}_k^{b,c} \le \ln\Big(P_{b,k}^{\max}\Big), \quad \forall b \in \mathcal{B}, \forall k \in \mathcal{K}, \quad (43)$$

$$\tilde{p}_l^d \le \ln(P_l^{\max}), \quad \forall l \in \mathcal{L}. \quad (44)$$

Note that **P1.2** is still non-convex when y, $\tilde{\mathbf{p}}^c$ and $\tilde{\mathbf{p}}^d$ are to be optimized jointly. Thus, we resort to employing an alternating optimization approach, where we can have two convex sub-problems since the constraints of **P1.2** are convex. First, by fixing $\tilde{\mathbf{p}}^c$ and $\tilde{\mathbf{p}}^d$, the objective function of **P1.2** becomes a concave quadratic function in terms of y since we always have $\mathrm{B}(\tilde{\mathbf{p}}^c, \tilde{\mathbf{p}}^d) > 0$. Therefore, the sub-problem of finding y is always convex for fixed transmit powers. Also by fixing y, the objective function becomes jointly concave in $\tilde{\mathbf{p}}^c$ and $\tilde{\mathbf{p}}^d$ since $\sqrt{\mathrm{A}(\tilde{\mathbf{p}})}$ and $-\mathrm{B}(\tilde{\mathbf{p}})$ are both concave functions. Note that the summation of two concave functions are also concave. Consequently, the power allocation sub-problem will be convex for fixed y as well.

By applying the explained alternating optimization approach, we propose the following iterative algorithm to solve **P1.2**. First let us initialize $\tilde{\mathbf{p}}^c = \tilde{\mathbf{p}}_o^c$ and $\tilde{\mathbf{p}}^d = \tilde{\mathbf{p}}_o^d$, and solve for y of which the optimal result can be obtained analytically as

$$y_o^* = \frac{\sqrt{\mathrm{A}\big(\tilde{\mathbf{p}}_o^c, \tilde{\mathbf{p}}_o^d\big)}}{\mathrm{B}\big(\tilde{\mathbf{p}}_o^c, \tilde{\mathbf{p}}_o^d\big)}, \quad (45)$$

where o is the index of outer iteration. Next, fixing y_o^*, we solve for $\tilde{\mathbf{p}}^c$ and $\tilde{\mathbf{p}}^d$, which is a constrained convex optimization problem. We iteratively solve for $\tilde{\mathbf{p}}^c$ and $\tilde{\mathbf{p}}^d$, and y until a stopping criterion is met, which is either a maximum number of iterations or minimum difference of values of y in two subsequent iterations. Note that, in practice, the maximum number of iterations is set according to practical limitations such as computational complexity and delay constraints. The whole procedure is summarized in Algorithm 1, where $\delta_{y,min}$ is the minimum absolute difference of values of y in two subsequent iterations and $iter_{max}$ is the maximum number of iterations.

Algorithm 1 Proposed Energy Efficiency Optimization (EEO) Algorithm

Input: Large-scale fading coefficients, P_k^{max}, P_l^{max} and pilot powers.

Output: $\tilde{\mathbf{p}}^c$ and $\tilde{\mathbf{p}}^d$.

Initialization : $i = 1$, $\tilde{\mathbf{p}}_o^c = P_k^{max}, \tilde{\mathbf{p}}_o^l = P_l^{max}$

while $i \le iter_{max}$ or $\delta_y \ge \delta_{y,min}$ **do**

  Solve **P1.2** to find the optimized values of $\tilde{\mathbf{p}}^c$ and $\tilde{\mathbf{p}}^d$,

  Update $\eta_{b,k}^c = \frac{\overline{\mathrm{SINR}}_k^{b,c}}{\overline{\mathrm{SINR}}_k^{b,c}+1}, \eta_l^d = \frac{\overline{\mathrm{SINR}}_l^d}{\overline{\mathrm{SINR}}_l^d+1}$,

  Update $\zeta_{b,k}^c = \ln(1 + \overline{\mathrm{SINR}}_k^{b,c}) - \eta_{b,k}^c \ln(\overline{\mathrm{SINR}}_k^{b,c}), \zeta_l^d = \ln(1 + \overline{\mathrm{SINR}}_l^d) - \eta_l^d \ln(\overline{\mathrm{SINR}}_l^d)$,

  Calculate $\mathrm{A}(\tilde{\mathbf{p}}_i^c, \tilde{\mathbf{p}}_i^d)$ and $\mathrm{B}(\tilde{\mathbf{p}}_i^c, \tilde{\mathbf{p}}_i^d)$,

  Update the auxiliary variable $y_i = \frac{\sqrt{\mathrm{A}(\tilde{\mathbf{p}}_i^c, \tilde{\mathbf{p}}_i^d)}}{\mathrm{B}(\tilde{\mathbf{p}}_i^c, \tilde{\mathbf{p}}_i^d)}$,

  Compute $\delta_y = |y_i - y_{i-1}|$, $i = i + 1$,

end while

return The optimized values of $\tilde{\mathbf{p}}^c$ and $\tilde{\mathbf{p}}^d$.

TABLE III
SIMULATION PARAMETERS

Parameter	Default value
Number of BS antennas (M)	100
Number of cells (B)	4
Number of D2D pairs (L)	10
Number of CUs at each cell (K)	4
Maximum CU transmit power ($P_{\text{max}}^{\text{CU}}$)	2 mW
Maximum D2D transmit power ($P_{\text{max}}^{\text{D2D}}$)	0.2 mW
CU Rician factor (K_{CU})	10 dB
D2D Rician factor (K_{D2D})	10 dB
CU pilot power ($P_{\text{pilot}}^{\text{CU}}$)	2 mW
D2D pilot power ($P_{\text{pilot}}^{\text{D2D}}$)	0.2 mW
Shadowing parameter	5 dB
Distance of D2D pairs (D)	20 m
D2D circuit power consumption ($p_l^{d,ci}$)	0.025 mW
CU circuit power consumption ($p_{b,k}^{c,ci}$)	0.2 mW
White noise variance σ^2	-91 dBm
Path loss model for CU links	$128.1 + 35\log_{10}(d)$
Path loss model for D2D links	$148.1 + 40\log_{10}(d)$
Minimum absolute difference of values of y in two subsequent iterations ($\delta_{y,min}$)	10^{-4}

V. NUMERICAL RESULTS

In this section, we investigate the EE performance of the system utilizing the proposed EE optimization algorithm. Table III shows the default values for the parameters of the network, where d is the distance between the transmitter and receiver.

We considered a network in a 2 km by 2 km area with $B = 4$ cells such that each BS has 1 km^2 squared-shape coverage area. A typical BS with M antennas serves $K = 4$ CUs in UL. The D2D pairs are randomly located in the whole network area. Also, the CU and D2D devices are positioned based on the Poisson point process (PPP) methodology. The Monte Carlo simulation results are obtained for 500 realizations of different coordinates of devices (D2D pairs and CUs) distributed over the network under PPP model, except for the D2D receivers which are distributed at a fixed distance from their associated transmitters. Next, the cumulative distribution function (CDF) curves are plotted for the acquired dataset.

First, we illustrate the effect of increasing CU LOS component K_{CU} (with their own serving BSs) in Fig. 3a, where the EE is obtained according to (34). It can be seen that increasing K_{CU} from -100 dB to 30 dB results in about

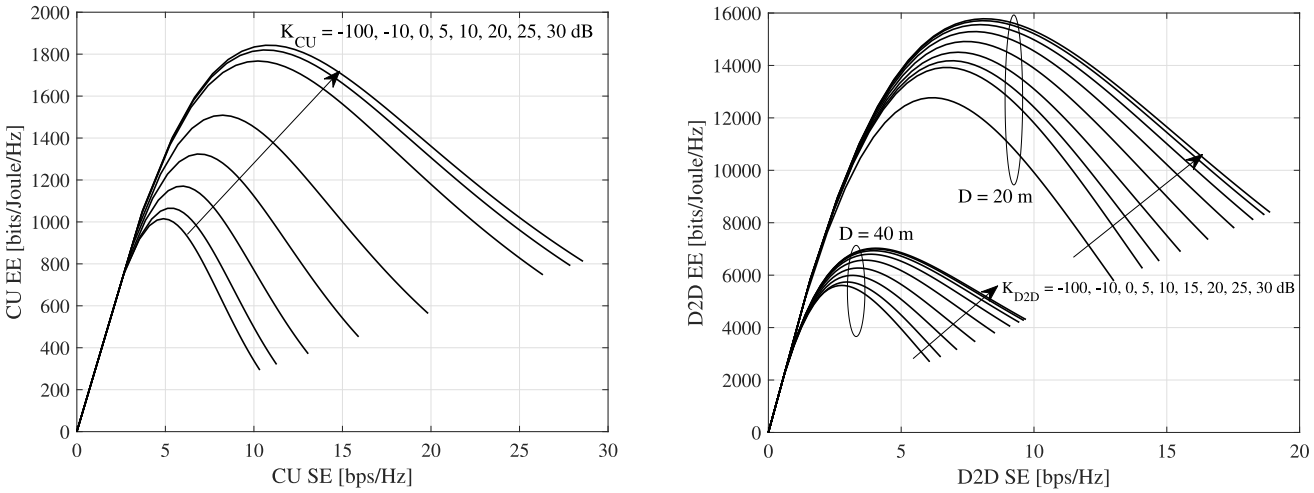

Fig. 3. (a): The EE vs. total SE of the CUs. (b): The EE vs. total SE of the D2D pairs. Note the impact of increasing K_{D2D} on the EE of all D2D pairs.

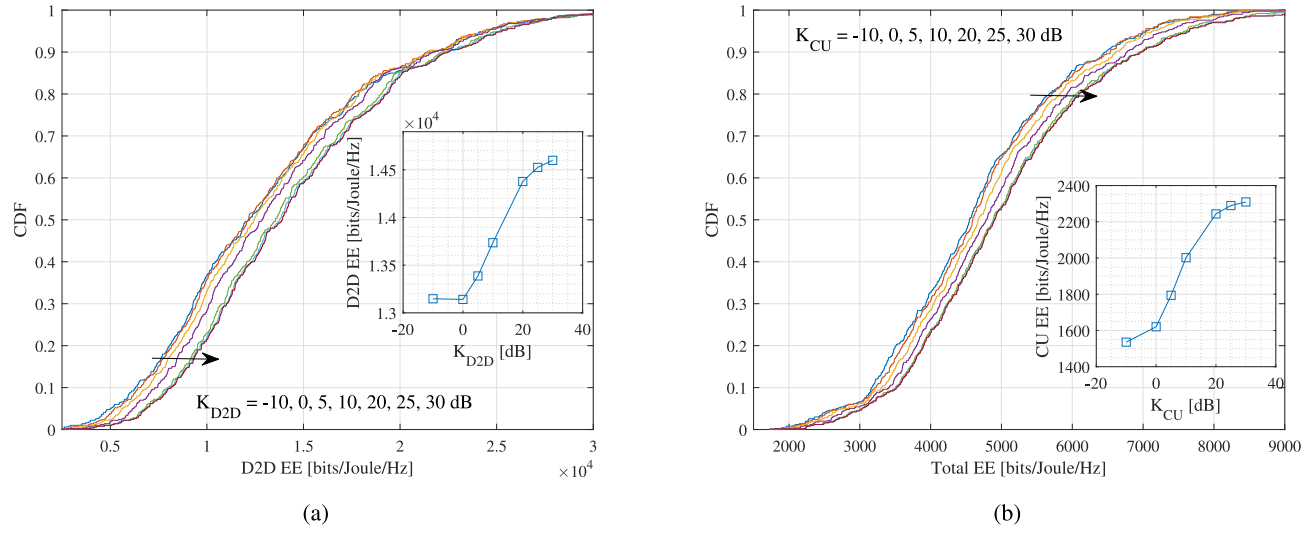

Fig. 4. (a): The impact of increasing K_{D2D} on the optimized EE of all D2D pairs. (b): The optimized EE CDF curves in terms of increasing K_{CU}.

1000 bits/Joule/Hz improvement in the maximum EE of CUs and 5 bps/Hz (90%) in its corresponding SE. Note that $K_{\mathrm{CU}} = -\infty$ dB and $K_{\mathrm{D2D}} = -\infty$ dB is a special case corresponding to the Rayleigh fading which was discussed in [25]. Next, we illustrate the EE curves for D2D pairs in Fig. 3b. It is shown that when the distance of D2D pairs reduces, the EE increases which is an intuitive result. Furthermore, we observe that as the LOS component of the D2D users K_{D2D} increases, the maximum EE value goes higher. More precisely, for the case of $D = 20$m by varying K_{D2D} from -100 dB to 30 dB, an increase of about 20% and 25% on the maximum EE and the corresponding SE is observed. Comparing the results in Fig. 3a and Fig. 3b, we can conclude that having a strong LOS component is less critical in D2D pairs as compared to CUs. However, it can still lead to a significant improvement in D2D and CU networks' performance.

Next, we discuss the EE optimizations of the D2D devices. Fig. 4a shows the CDF of the EE of D2D pairs for $D = 20m$, which has a similar trend as the results of previous analytical expressions. According to Fig. 4a, the D2D EE is less than or equal to 25000 bits/Joule/Hz for all K_{D2D} values with a probability of 95%. We can also observe that the D2D EE saturates at the K_{D2D} of around 30 dB. Fig. 4b shows the effect of increasing K_{CU} on the total EE of the system (cellular and D2D), which shows a similar trend as in Fig. 3a. We can observe that for all K_{CU} values, the total EE is less than or equal to 8000 bits/Joule/Hz with a probability of about 97%. Also, the total EE saturates at the K_{CU} of about 30 dB.

On the other side, Fig. 5 shows the trade-off between the optimized EEs of CUs and D2D pairs. It can be seen that as K_{D2D} increases the optimized EE of D2D pairs increases as well, while the optimized EE of CUs decreases. For instance, as K_{D2D} increases from -10 dB to 30 dB, the optimized D2D EE increases by about 10%, while the optimized CU EE has a decrease of about 5%. This result confirms that the performance of CUs are less affected by changing the LOS factor of D2D pairs K_{D2D}. However, the D2D pairs' performance is more

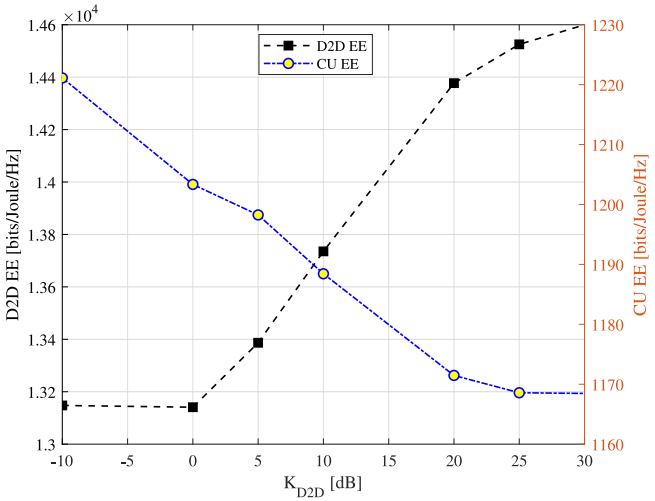

Fig. 5. The trade-off region of the increasing K_{D2D} on the optimized EE all D2D pairs and CUs.

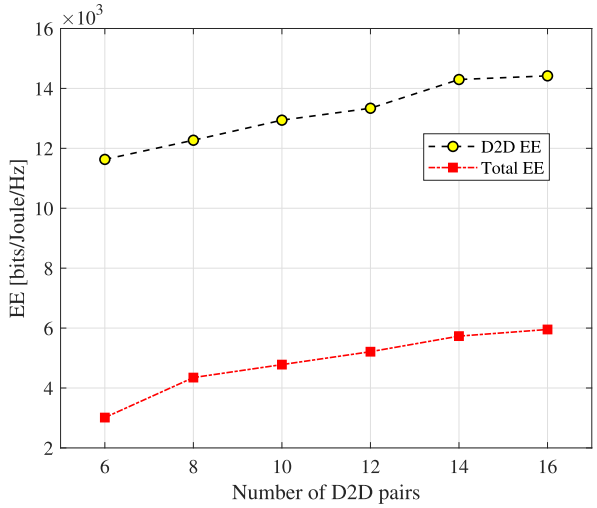

Fig. 6. The impact of the number of D2D pairs on the D2D EE, and the total EE.

influenced by having a stronger LOS channel with their receivers.

The impact of the number of D2D pairs (D2D users' density) on the D2D EE as well as the total EE is illustrated in Fig. 6. The total EE is calculated as the ratio of the sum of all the achievable SEs in the system over the total transmit power and circuitry power consumption. Similarly, the D2D EE is obtained by dividing the total D2D SE in the network by total transmit power and circuitry power consumption of D2D pairs. It is observed that as the number of D2D pairs increases, the D2D' EE and the total EEs go higher as well. This highlights the applicability of our proposed EE maximization approach as a scalable approach in terms of increasing the total number of D2D pairs. In addition, the total EE is lower than the D2D EE since the D2D network usually has better EE performance than the cellular network due to having lower power consumption while acquiring higher data rate thanks to short distance communications.

VI. Conclusion

In this paper, a detailed analysis for a lower-bound on the SE in an underlaid D2D multi-cell m-MIMO was presented over a Rician fading channel. Closed-form expressions were obtained for the CU SE employing MMSE channel estimation technique. Then, we provided a closed-form approximate expression for the ergodic capacity of the D2D pairs when a LOS component is present between Tx/Rx pairs due to the short distance communication. We also provided an algorithm to maximize the EE performance of the network. To this end, we first formulated the EE optimization problem where the transmit power of CUs and D2D devices were to be optimized. To solve the problem, a fractional programming technique was employed and the reformulated problem was solved via an alternating optimization approach. Simulation results showed that by properly designing transmit power of the users, the network EE can be significantly improved. Also, it was demonstrated that having strong LOS components enhances the performance of both D2D pairs and CUs. As a future work, the results can be extended to more practical setups; e.g., under different hardware imperfections at the BSs or at the user sides such as finite resolution digital-to-analog converters (DACs). Also, the results can be extended to the case where the CUs or the D2D pairs have multiple antennas to highlight the significance of underlying D2D communications in multi-cell m-MIMO systems in increasing the total EE as well as the SE of the network.

Appendix A
Proof of Proposition 1

We know that if an observation $\mathbf{y} = \sum_{b=1} x_b \boldsymbol{\zeta}_b + \boldsymbol{\omega} \in \mathbb{C}^{N\times 1}$ is given in terms of unknown parameters $\boldsymbol{\zeta_b} \in \mathbb{C}^{N\times 1}$, coefficients x_n and a noise vector $\boldsymbol{\omega} \in \mathbb{C}^{N\times 1}$, the MMSE estimation $\hat{\boldsymbol{\zeta}}_b$ can be expressed as the conditional expectation of $\boldsymbol{\zeta}_b$ given $\mathbf{y}$, i.e.,

$$\hat{\boldsymbol{\zeta}}_b = \mathbb{E}[\boldsymbol{\zeta}_b|\mathbf{y}] = \mathbb{E}[\boldsymbol{\zeta}_b] + \mathbf{C}_{\boldsymbol{\zeta}_b\mathbf{y}}\mathbf{C}_{\mathbf{yy}}^{-1}(\mathbf{y} - \mathbb{E}[\mathbf{y}]), \tag{46}$$

where $\mathbf{C}_{\boldsymbol{\zeta}_b\mathbf{y}}$, $\mathbf{C}_{\mathbf{y}}$ are the cross-covariance matrices between $\mathbf{y}$ and $\boldsymbol{\zeta}_b$, and the auto-covariance matrix of $\mathbf{y}$, respectively [37]. After the projection of the received signals on the transmitted pilot sequences, the channel estimates are obtained by substituting $x_b = \sqrt{\tau p_{b,k}^{p,c}}$, $x_{b'} = \sqrt{\tau p_{b',c}^{b,c}(K_{b'k}+1)}$, $\boldsymbol{\zeta}_b = \mathbf{h}_{b,k,\mathrm{NLOS}}^{b,c}$, and $\boldsymbol{\zeta}_{b'} = \mathbf{h}_{b',k,\mathrm{NLOS}}^{b,c}$ $(b \neq b')$ in (46) which corresponds to the result in (6). This completes the proof.

Appendix B
Proof of Theorem 1

The processed received data signal of the CU k at b-th cell by exploiting use and then forget (UATF) technique is given by

$$\left(\hat{\mathbf{h}}_{b,k}^{b,c}\right)^H \mathbf{y}_b^c = \sqrt{p_{b,k}^c}\mathbb{E}\left[\left(\hat{\mathbf{h}}_{b,k}^{b,c}\right)^H \mathbf{h}_{b,k}^{b,c}\right] s_{b,k}^c + \sqrt{p_{b,k}^c}\left(\left(\hat{\mathbf{h}}_{b,k}^{b,c}\right)^H \mathbf{h}_{b,k}^{b,c} - \mathbb{E}\left[\left(\hat{\mathbf{h}}_{b,k}^{b,c}\right)^H \mathbf{h}_{b,k}^{b,c}\right]\right) s_{b,k}^c$$

$$+\sum_{k'=1,k'\neq k}^{K}\sqrt{p_{b,k'}^{c}}\left(\hat{\mathbf{h}}_{b,k}^{b,c}\right)^{H}\mathbf{h}_{b,k'}^{b,c}s_{b,k'}^{c}+\sum_{b'=1,b'\neq b}^{B}\sum_{k'=1,k'\neq k}^{K}\sqrt{p_{b',k'}^{c}}\left(\hat{\mathbf{h}}_{b,k}^{b,c}\right)^{H}\mathbf{h}_{b',k'}^{b,c}s_{b',k'}^{c}+\sum_{l=1}^{L}\sqrt{p_{l}^{d}}\left(\hat{\mathbf{h}}_{b,k}^{b,c}\right)^{H}\mathbf{h}_{l}^{b,d}s_{l}^{d}+\left(\hat{\mathbf{h}}_{b,k}^{b,c}\right)^{H}\mathbf{w}_{b}, \tag{47}$$

where the first term is the receiver knowledge of the user signal and the other components are considered as the interference plus noise signals. Since Gaussian noise is the worst additive uncorrelated noise, its achievable rate is less than any other uncorrelated noise with the same mean and variance. Then, as the achievable rate of uncorrelated Gaussian noise is equal to $\log_2(1+\text{SINR})$, (21) provides a lower-bound on the achievable rate, where the SINR of the k-th CU in the b-th cell is given in (48), shown at the bottom of the page.

In the following, we calculate the nominator and denominator of (48). After some straightforward mathematical manipulations and computing the expectations we will have

$$\left|\mathbb{E}\left[\left(\hat{\mathbf{h}}_{b,k}^{b,c}\right)^{H}\mathbf{h}_{b,k}^{b,c}\right]\right|^{2}=M^{2}\left(\beta_{b,k}^{b,c}\right)^{2}, \tag{49}$$

$$\mathbb{E}\left[\left|\left(\hat{\mathbf{h}}_{b,k}^{b,c}\right)^{H}\mathbf{h}_{b,k}^{b,c}\right|^{2}\right]=M^{2}\left(\beta_{b,k}^{b,c}\right)^{2}+M\left(\beta_{b,k}^{b,c}\right)^{2}\frac{K_{bk}}{(K_{bk}+1)^{2}}+\frac{M\beta_{b,k}^{b,c}\left(\sum_{b'=1,b'\neq b}^{B}\tau p_{b',k}^{p,c}(K_{b'k}+1)\beta_{b',k}^{b,c}+1\right)}{(K_{bk}+1)\tau p_{b,k}^{p,c}}, \tag{50}$$

$$\begin{aligned}\mathcal{I}_{k',b}^{k'\neq k}&=\mathbb{E}\left[\left|\left(\hat{\mathbf{h}}_{b,k}^{b,c}\right)^{H}\mathbf{h}_{b,k'}^{b,c}\right|^{2}\right]\\&=\beta_{b,k}^{b,c}\beta_{b,k'}^{b,c}\frac{K_{bk}K_{bk'}\phi_{kk'}^{2}+M(K_{bk}+K_{bk'})+M}{(K_{bk'}+1)(K_{bk}+1)}+M\beta_{b,k}^{b,c}\frac{\sum_{b'=1,b'\neq b}^{B}\tau p_{b',k}^{p,c}(K_{b'k}+1)\beta_{b,k'}^{b,c}+1}{\tau p_{b,k}^{p,c}(K_{bk}+1)},\end{aligned} \tag{51}$$

$$\begin{aligned}\mathcal{I}_{k,b'}^{b'\neq b}&=\mathbb{E}\left[\left|\left(\hat{\mathbf{h}}_{b,k}^{b,c}\right)^{H}\mathbf{h}_{b',k}^{b,c}\right|^{2}\right]\\&=M^{2}\left(\beta_{b',k}^{b,c}\right)^{2}\frac{\tau p_{b',k}^{p,c}(K_{b'k}+1)}{\tau p_{b,k}^{p,c}(K_{bk}+1)}+M\beta_{b,k}^{b,c}\beta_{b',k}^{b,c}+M\beta_{b',k}^{b,c}\frac{\sum_{b''=1,b''\neq b}^{B}\tau p_{b'',k}^{p,c}(K_{b''k}+1)\beta_{b'',k}^{b,c}+1}{\tau p_{b,k}^{p,c}(K_{bk}+1)},\end{aligned} \tag{52}$$

$$\begin{aligned}\mathcal{I}_{k',b'}^{k'\neq k,b'\neq b}&=\mathbb{E}\left[\left|\left(\hat{\mathbf{h}}_{b,k}^{b,c}\right)^{H}\mathbf{h}_{b',k'}^{b,c}\right|^{2}\right]\\&=M\beta_{b',k'}^{b,c}\beta_{b,k}^{b,c}+M\beta_{b',k'}^{b,c}\frac{\sum_{b''=1,b''\neq b}^{B}\tau p_{b'',k}^{p,c}(K_{b''k}+1)\beta_{b'',k}^{b,c}+1}{\tau p_{b,k}^{p,c}(K_{bk}+1)},\end{aligned} \tag{53}$$

$$\mathbb{E}\left[\left|\hat{\mathbf{h}}_{b,k}^{b,c}\right|_{2}^{2}\right]=M\beta_{b,k}^{b,c}+M\frac{\sum_{b'=1,b'\neq b}^{B}\tau p_{b',k}^{p,c}(K_{b'k}+1)\beta_{b',k}^{b,c}+1}{\tau p_{b,k}^{p,c}(K_{bk}+1)}, \tag{54}$$

where $\phi_{kk'}=\frac{\sin(0.5M\pi(\sin\theta_{bk}-\sin\theta_{bk'}))}{\sin(0.5\pi(\sin\theta_{bk}-\sin\theta_{bk'}))}$.

Also, the interference term from D2D transmitters is expressed as

$$\begin{aligned}\mathcal{I}_{l}&=\mathbb{E}\left[\left|\left(\hat{\mathbf{h}}_{b,k}^{b,c}\right)^{H}\mathbf{h}_{l}^{b,d}\right|^{2}\right]=\mathbb{E}\left[\left(\hat{\mathbf{h}}_{b,k}^{b,c}\right)^{H}\mathbf{h}_{l}^{b,d}\left(\mathbf{h}_{l}^{b,d}\right)^{H}\hat{\mathbf{h}}_{b,k}^{b,c}\right]\\&=\beta_{l}^{b,d}\mathbb{E}\left[\left(\hat{\mathbf{h}}_{b,k}^{b,c}\right)^{H}\mathbf{I}_{M\times M}\hat{\mathbf{h}}_{b,k}^{b,c}\right]\\&=\beta_{l}^{b,d}\left(M\beta_{b,k}^{b,c}+M\frac{\sum_{b'=1,b'\neq b}^{B}\tau p_{b',k}^{p,c}(K_{b'k}+1)\beta_{b',k}^{b,c}+1}{\tau p_{b,k}^{p,c}(K_{bk}+1)}\right).\end{aligned} \tag{55}$$

Finally, after substituting the mathematical expressions in the SINR formula given in (48) we conclude (22).

Appendix C
Proof of Theorem 2

The lower-bound for capacity C of fading channel ϑ with side information Ω and non-Gaussian noise n is given by [36]

$$C\geq\tilde{C}=\mathbb{E}_{\Omega}\left[\log_2\left(1+\frac{\rho|\mathbb{E}[\vartheta|\Omega]|^{2}}{\rho\mathbb{V}[\vartheta|\Omega]+\mathbb{V}[n|\Omega]}\right)\right], \tag{56}$$

where n and ρ are the additive noise with arbitrary distribution and the transmit power, respectively. By employing (56) and (17), the lower-bound on the capacity for D2D receiver l is given in (57), shown at the top of the next page, where DP_l and IP_l denote the desired signal power and the interference power, respectively. The capacity lower-bound in (57) is intractable. Therefore, employing approximation $\mathbb{E}[\log_2(1+\frac{X}{Y})]\approx\log_2(1+\frac{\mathbb{E}[X]}{\mathbb{E}[Y]})$ for non-negative random variables X and Y, we have

$$\tilde{C}_{l}^{d}\approx\log_2\left(1+\frac{\mathbb{E}_{\Omega}[\text{DP}_l]}{\mathbb{E}_{\Omega}[\text{IP}_l]}\right), \tag{58}$$

where after computing the inner terms DP_l, IP_l and taking outer expectation with respect to side information Ω in

$$\text{SINR}_{k}^{b,c}=\frac{p_{b,k}^{c}\left|\mathbb{E}\left[\left(\hat{\mathbf{h}}_{b,k}^{b,c}\right)^{H}\mathbf{h}_{b,k}^{b,c}\right]\right|^{2}}{\sum_{b'=1}^{B}\sum_{k'=1}^{K}p_{b',k'}^{c}\mathbb{E}\left[\left|\left(\hat{\mathbf{h}}_{b,k}^{b,c}\right)^{H}\mathbf{h}_{b',k'}^{b,c}\right|^{2}\right]-p_{b,k}^{c}\left|\mathbb{E}\left[\left(\hat{\mathbf{h}}_{b,k}^{b,c}\right)^{H}\mathbf{h}_{b,k}^{b,c}\right]\right|^{2}+\sum_{l=1}^{L}p_{l}^{d}\mathbb{E}\left[\left|\left(\hat{\mathbf{h}}_{b,k}^{b,c}\right)^{H}\mathbf{h}_{l}^{b,d}\right|^{2}\right]+\mathbb{E}\left[\left|\hat{\mathbf{h}}_{b,k}^{b,c}\right|_{2}^{2}\right]} \tag{48}$$

$$\tilde{C}_l^d = \mathbb{E}_\Omega\left[\log_2\left(1+\frac{\overbrace{\frac{p_l^d}{K_l+1}\mathbb{E}\left[\left|\sqrt{K_l}\bar{g}_l^{l,d}+\hat{g}_{l,\mathrm{NLOS}}^{l,d}\right|^2|\Omega\right]}^{\mathrm{DP}_l}}{\underbrace{p_l^d\mathbb{V}\left[g_l^{l,d}|\Omega\right]+\mathbb{V}\left[\sum_{b=1}^{B}\sum_{k=1}^{K}\sqrt{p_{b,k}^{l,c}}g_{b,k}^{l,c}s_{b,k}^c+\sum_{l'=1,l'\neq l}^{L}\sqrt{p_{l'}^d}g_{l'}^{l,d}s_{l'}^d+w_l|\Omega\right]}_{\mathrm{IP}_l}}\right)\right] \tag{57}$$

terms of imperfect channel estimates, the expected values are given by

$$\mathbb{E}_\Omega[\mathrm{DP}_l] = \frac{p_l^d}{K_l+1}\left(K_l\beta_l^{l,d}+\gamma_l^{l,d}\right), \tag{59}$$

$$\mathbb{E}_\Omega[\mathrm{IP}_l] = \frac{p_l^d\left(\beta_l^{l,d}-\gamma_l^{l,d}\right)}{K_l+1}+\sum_{b=1}^{B}\sum_{k=1}^{K}p_{b,k}^c\beta_{l,c}^{b,k} + \sum_{l'=1,l'\neq l}^{L}p_{l'}^d\beta_{l'}^{l,d}+1, \tag{60}$$

which concludes the proof.

REFERENCES

[1] A. Asadi, Q. Wang, and V. Mancuso, "A survey on device-to-device communication in cellular networks," *IEEE Commun. Surveys Tuts.*, vol. 16, no. 4, pp. 1801–1819, 4th Quart., 2014.

[2] L. Wang and H. Tang, *Device-to-Device Communications in Cellular Networks*. Cham, Switzerland: Springer, 2016.

[3] S. Zhang, J. Liu, H. Guo, M. Qi, and N. Kato, "Envisioning device-to-device communications in 6G," *IEEE Netw.*, vol. 34, no. 3, pp. 86–91, May/Jun. 2020.

[4] F. Jameel, Z. Hamid, F. Jabeen, S. Zeadally, and M. A. Javed, "A survey of device-to-device communications: Research issues and challenges," *IEEE Commun. Surveys Tuts.*, vol. 20, no. 3, pp. 2133–2168, 3rd Quart., 2018.

[5] M. Salehi, A. Mohammadi, and M. Haenggi, "Analysis of D2D underlaid cellular networks: SIR Meta distribution and mean local delay," *IEEE Trans. Commun.*, vol. 65, no. 7, pp. 2904–2916, Jul. 2017.

[6] N. Zabetian, A. Mohammadi, and M. Masoudi, "Energy-efficient power allocation for device-to-device communications underlaid cellular networks using stochastic geometry," *Trans. Emerg. Telecommun. Technol.*, vol. 30, no. 12, 2019, Art. no. e3768.

[7] N. Zabetian, A. Mohammadi, and M. Kazemi, "Energy efficiency optimization for device-to-device communication underlaying cellular networks in millimeter-wave," *Int. J. Commun. Syst.*, vol. 33, no. 6, 2020, Art. no. e4287.

[8] Y. Pan, C. Pan, Z. Yang, and M. Chen, "Resource allocation for D2D communications underlaying a NOMA-based cellular network," *IEEE Wireless Commun. Lett.*, vol. 7, no. 1, pp. 130–133, Feb. 2018.

[9] Z. Yang, N. Huang, H. Xu, Y. Pan, Y. Li, and M. Chen, "Downlink resource allocation and power control for device-to-device communication underlaying cellular networks," *IEEE Commun. Lett.*, vol. 20, no. 7, pp. 1449–1452, Jul. 2016.

[10] G. Fodor *et al.*, "Design aspects of network assisted device-to-device communications," *IEEE Commun. Mag.*, vol. 50, no. 3, pp. 170–177, Mar. 2012.

[11] J. Liu, Y. Kawamoto, H. Nishiyama, N. Kato, and N. Kadowaki, "Device-to-device communications achieve efficient load balancing in LTE-advanced networks," *IEEE Wireless Commun.*, vol. 21, no. 2, pp. 57–65, Apr. 2014.

[12] D. Feng, L. Lu, Y. W. Yi, G. Y. Li, G. Feng, and S. Li, "Device-to-device communications underlaying cellular networks," *IEEE Trans. Commun.*, vol. 61, no. 8, pp. 3541–3551, Aug. 2013.

[13] H. Xu, W. Xu, Z. Yang, J. Shi, and M. Chen, "Pilot reuse among D2D users in D2D underlaid massive MIMO systems," *IEEE Trans. Veh. Technol.*, vol. 67, no. 1, pp. 467–482, Jan. 2018.

[14] Y. Liu, C. Pan, L. You, and W. Han, "D2D-enabled user cooperation in massive MIMO," *IEEE Syst. J.*, vol. 14, no. 3, pp. 4406–4417, Sep. 2020.

[15] S. Shalmashi, E. Björnson, M. Kountouris, K. W. Sung, and M. Debbah, "Energy efficiency and sum rate tradeoffs for massive MIMO systems with underlaid device-to-device communications," *Eurasip J. Wireless Commun. Netw.*, vol. 2016, no. 1, pp. 1–18, 2016.

[16] X. Liu, Y. Li, X. Li, L. Xiao, and J. Wang, "Pilot reuse and interference-aided MMSE detection for D2D underlay massive MIMO," *IEEE Trans. Veh. Technol.*, vol. 66, no. 4, pp. 3116–3130, Apr. 2017.

[17] Z. Zhang, Y. Li, R. Wang, and K. Huang, "Rate adaptation for Downlink massive MIMO networks and underlaid D2D links: A learning approach," *IEEE Trans. Wireless Commun.*, vol. 18, no. 3, pp. 1819–1833, Mar. 2019.

[18] H. Echigo and T. Ohtsuki, "Graph coloring-based pilot reuse with AOA and distance in D2D underlay massive MIMO," in *Proc. IEEE 87th Veh. Technol. Conf. (VTC Spring)*, 2018, pp. 1–6.

[19] H. Xu, N. Huang, Z. Yang, J. Shi, B. Wu, and M. Chen, "Pilot allocation and power control in D2D underlay massive MIMO systems," *IEEE Commun. Lett.*, vol. 21, no. 1, pp. 112–115, Jan. 2017.

[20] X. Qiao, Y. Zhang, M. Zhou, L. Yang, and H. Zhu, "Downlink achievable rate of D2D underlaid cell-free massive MIMO systems with low-resolution DACs," *IEEE Syst. J.*, early access, Aug. 11, 2021, doi: 10.1109/JSYST.2021.3098926.

[21] H. Masoumi, M. J. Emadi, and S. Buzzi, "Coexistence of D2D communications and cell-free massive MIMO systems with low resolution ADC for improved throughput in beyond-5G networks," *IEEE Trans. Commun.*, vol. 70, no. 2, pp. 999–1013, Feb. 2022.

[22] A. He, L. Wang, Y. Chen, K. K. Wong, and M. Elkashlan, "Spectral and energy efficiency of uplink D2D underlaid massive MIMO cellular networks," *IEEE Trans. Commun.*, vol. 65, no. 9, pp. 3780–3793, Sep. 2017.

[23] P. Liu, K. Luo, D. Chen, T. Jiang, and M. Matthaiou, "Spectral efficiency analysis of multi-cell massive MIMO systems with Ricean fading," in *Proc. 10th Int. Conf. Wireless Commun. Signal Process. (WCSP)*, 2018, pp. 1–7.

[24] X. Lin, R. W. Heath, and J. G. Andrews, "The interplay between massive MIMO and underlaid D2D networking," *IEEE Trans. Wireless Commun.*, vol. 14, no. 6, pp. 3337–3351, Jun. 2015.

[25] A. Ghazanfari, E. Bjornson, and E. G. Larsson, "Optimized power control for massive MIMO with underlaid D2D communications," *IEEE Trans. Commun.*, vol. 67, no. 4, pp. 2763–2778, Apr. 2019.

[26] X. Nie and F. Zhao, "Pilot allocation and power optimization of massive MIMO cellular networks with underlaid D2D communications," *IEEE Internet Things J.*, vol. 8, no. 20, pp. 15317–15333, Oct. 2021.

[27] P. Mach, T. Spyropoulos, and Z. Becvar, "Incentive-based D2D relaying in cellular networks," *IEEE Trans. Commun.*, vol. 69, no. 3, pp. 1775–1788, Mar. 2021.

[28] L. Sanguinetti, A. Kammoun, and M. Debbah, "Theoretical performance limits of massive MIMO with uncorrelated Rician fading channels," *IEEE Trans. Commun.*, vol. 67, no. 3, pp. 1939–1955, Mar. 2019.

[29] Y. J. Chun, S. L. Cotton, H. S. Dhillon, A. Ghrayeb, and M. O. Hasna, "A stochastic geometric analysis of device-to-device communications operating over generalized fading channels," *IEEE Trans. Wireless Commun.*, vol. 16, no. 7, pp. 4151–4165, Jul. 2017.

[30] M. Peng, Y. Li, T. Q. Quek, and C. Wang, "Device-to-device underlaid cellular networks under Rician fading channels," *IEEE Trans. Wireless Commun.*, vol. 13, no. 8, pp. 4247–4259, Aug. 2014.

[31] M. R. Mili, A. Khalili, N. Mokari, S. Wittevrongel, D. W. K. Ng, and H. Steendam, "Tradeoff between ergodic energy efficiency and spectral efficiency in D2D communications under Rician fading channel," *IEEE Trans. Veh. Technol.*, vol. 69, no. 9, pp. 9750–9766, Sep. 2020.
[32] C. Vallati, A. Virdis, E. Mingozzi, and G. Stea, "Exploiting LTE D2D communications in M2M fog platforms: Deployment and practical issues," in *Proc. IEEE 2nd World Forum Internet of Things (WF-IoT)*, 2015, pp. 585–590.
[33] B. Coll-Perales, J. Gozalvez, and J. L. Maestre, "5G and beyond: Smart devices as part of the network fabric," *IEEE Netw.*, vol. 33, no. 4, pp. 170–177, Jul./Aug. 2019.
[34] Q. Zhang, S. Jin, K.-K. Wong, H. Zhu, and M. Matthaiou, "Power scaling of uplink massive MIMO systems with arbitrary-rank channel means," *IEEE J. Sel. Topics Signal Process.*, vol. 8, no. 5, pp. 966–981, Oct. 2014.
[35] Q. Zhang, S. Jin, Y. Huang, and H. Zhu, "Uplink rate analysis of multicell massive MIMO systems in Ricean fading," in *Proc. IEEE Global Commun. Conf.*, 2014, pp. 3279–3284.
[36] T. L. Marzetta and H. Q. Ngo, *Fundamentals of Massive MIMO*. Cambridge, U.K.: Cambridge Univ. Press, 2016.
[37] S. M. Kay, *Fundamentals of Statistical Signal Processing: Estimation Theory*. Englewood Cliffs, NJ, USA: Prentice Hall PTR, 1993.
[38] J. Papandriopoulos and J. S. Evans, "SCALE: A low-complexity distributed protocol for spectrum balancing in multiuser DSL networks," *IEEE Trans. Inf. Theory*, vol. 55, no. 8, pp. 3711–3724, Aug. 2009.
[39] K. Shen and W. Yu, "Fractional programming for communication systems—Part I: Power control and beamforming," *IEEE Trans. Signal Process.*, vol. 66, no. 10, pp. 2616–2630, May 2018.

Ramin Hashemi (Graduate Student Member, IEEE) was born in Ardabil, Iran. He received the B.Sc. and M.Sc. degrees (Hons.) from the Amirkabir University of Technology (Tehran Polytechnic), Tehran, Iran, in 2016 and 2018, respectively. He is currently pursuing the Doctoral degree with the Center for Wireless Communications, University of Oulu, Finland, in the 6G Flagship project. His research interests include resource allocation in wireless networks, URLLC, RIS, MIMO wireless communications, beyond 5G, and fiber-optic communications.

Mohammad Kazemi (Member, IEEE) received the B.S. and M.S. degrees in electrical engineering from the K.N. Toosi University of Technology, Tehran, Iran, in 2007 and 2010, respectively, and the Ph.D. degree in electrical engineering from the Amirkabir University of Technology, Tehran, in 2017. He was a visiting student with Bilkent University, Turkey, in 2015. He was a Researcher of MMWCL with the Amirkabir University of Technology from 2017 to 2019. He is currently a Postdoctoral Fellow with the EE Department, Bilkent University. His research interests are in wireless communications and signal processing, with particular focus on massive MIMO and massive random access systems. He is currently the Editorial Assistant to the Editor-in-Chief of IEEE TRANSACTIONS ON COMMUNICATIONS.

Abbas Mohammadi (Senior Member, IEEE) received the B.Sc. degree in electrical engineering from Tehran University, Iran, in 1988, and the M.Sc. and Ph.D. degrees in electrical engineering from the University of Saskatchewan, Canada, in 1995 and 1999, respectively. In 1998, he joined Vecima Networks Inc., Victoria, Canada, as a Senior Research Engineer, where he researched wireless communications. Since March 2000, he has been with the Electrical Engineering Department, Amirkabir University of Technology (Tehran Polytechnic), Tehran, Iran, where he is currently a Professor. He has been an ICORE Visiting Professor with the Electrical and Computer Engineering Department, University of Calgary, Canada, and a Nokia Visiting Professor with the Tampere University of Technology, Finland. He has published over 200 journal and conference papers and holds three U.S. and one Canadian Patents. He has coauthored, *Six-port Technique with Microwave and Wireless Applications* (Artech House, 2009) and *RF Transceiver Design for MIMO Wireless Communications* (Springer, 2012). His current research interests include broadband wireless communications, adaptive modulation, MIMO systems, mesh and ad hoc networks, microwave and wireless subsystems, software design radio, and advanced wireless transceiver architectures.